analysis of radiation coupling from the tapered fiber is based on a meridional-ray-propagation model which includes power flow calculation with the Poynting vector. The simple meridional-ray model without modification is able to predict propagation delay and pulse dispersion of a step-index, multimode fiber.[5,6]

By reciprocity, it appears possible to utilize such a conically tapered fiber as a means of coupling light from sources with high numerical apertures into a fiber of a relatively small numerical aperture by entering through the tapered zone. Of course, no improvement of intrinsic source brightness is possible. In our application of this fiber as a dispersing element, it was found to be much simpler than any other scheme. Fibers which are normally bundled together for the purposes of directing light into remote regions for illumination might benefit from such a tapered end in order to achieve wide-angle illumination.

ACKNOWLEDGMENTS

This research was supported in part by National Institutes of Health Grant No. GM22550 (Burn Research Center). We would like to thank Professor Akira Ishimaru and Dr. Robert Smith for technical discussions. Computer programming assistance from Mr. W. K. Tsiang is also highly appreciated.

*Present address: Naval Ocean Systems Center, San Diego, Calif. 92152.

[1]P. K. Tien, G. Smolinsky, R. J. Martin, "Radiation fields of a tapered film and novel film-to-fiber coupler," *IEEE Transactions on Microwave Theory and Technology*, MTT-23, p. 79 (1975).

[2]M. P. Lisitsa, L. I. Berezhinskii, M. Y. Valakh, *Fiber Optics*, (Israel Program for Scientific Translations, New York, 1972), p. 36.

[3]D. Gloge, P. W. Smith, D. L. Bisbee, E. L. Chinnock, "Optical fiber end preparation for low-loss splices," Bell Sys. Tech. J., **52**, p. 1579 (1973).

[4]C. T. Chang, J. L. Bjorkstam, "Effect of nonuniform irradiance, and irradiance fluctuations, upon the response of photographic film," *J. Opt. Soc. Am.*, p. 1495 (1975).

[5]W. A. Gambling, J. P. Dakin, D. N. Payne, H. R. D. Sunk, "Propagation model for multimode optical-fibre waveguide," Electron. Lett., 8, p. 260 (May 1972).

[6]J. P. Dakin, W. A. Gambling, H. Matsumura, D. N. Payne, H. R. D. Sunk, "Theory of dispersion in lossless multimode optical fibres," Opt. Commun., **7**, p. 1 (1973).

Theory of Bragg fiber*

Pochi Yeh† and Amnon Yariv

California Institute of Technology, Pasadena, California 91125

Emanuel Marom

Hughes Research Laboratories, Malibu, California 90265

(Received 16 January 1978; revised manuscript received 24 May 1978)

The possibility of using Bragg reflection in a cylindrical fiber to obtain lossless confined propagation in a core with a *lower* refractive index than that of the cladding medium is proposed and analyzed.

I. INTRODUCTION

The guiding of light in a slab with a refractive index lower than that of the substrate was proposed and analyzed by Yeh and Yariv in 1976.[1] Experimental demonstration of this phenomenon in a sample fabricated by molecular beam epitaxy[2] was recently performed.[3] A general mode dispersion was derived for the planar Bragg waveguide with an arbitrary periodic layered medium as the substrate.[1,4] However, it is found that in order to get the best Bragg confinement, the periodic layered medium must consist of alternating quarter-wave layers.[5] This result is obtained by minimizing the outward flowing power in the guide. The same procedure will be applied in this paper to the cylindrical fiber.

Propagation of electromagnetic waves in cylindrically symmetric dielectric waveguides has become increasingly important in fiber optics communication. The guiding principle is similar to the planar slab waveguide. A dielectric fiber is capable of supporting confined modes provided the refractive index of the guiding region (core) is greater than that of the surroundings (cladding). This ensures the evanescent decay of optical waves as r goes to infinity. Instead of dealing with sine and cosine functions, one deals with Bessel functions of both kinds in the cylindrical regime. A great deal has been done on optical propagation in conventional fibers.[6–8]

In this paper we will show that, in principle, confined modes exist in a fiber with a low-index core, provided the core is surrounded by a suitably designed alternating cladding of high and low refractive indices (see Fig. 1). A fiber with this kind of cladding is called a Bragg fiber[9] and is similar in principle to the Bragg planar waveguide, where the light is guided by a low-index slab. To treat this problem properly we introduce an optimization similar to the one discussed in Ref. 5. Instead of solving for the confined modes of a given fiber structure, we search for the fiber structure such that the modes have some defined properties. The guiding of electromagnetic waves in a fiber with a low-index core, especially the hollow waveguide,[10] is not only important in optical communication, but also very useful in the guiding of uv or of soft x rays in a hollow Bragg cylindrical waveguide where almost any material is too lossy in that frequency regime. Another important application in fiber optics communication is the design of a

single-mode fiber. We have shown that a single-mode Bragg waveguide can be designed with a guiding layer thickness much larger than a wavelength.

A similar conclusion is derived for cylindrical Bragg waveguides. A single-mode fiber is capable of transmitting a light pulse without broadening due to modal dispersion.[11] Pulse broadening is a serious problem in digital fiber optics communication; where it places a limit on pulse repetition rate.

II. MATRIX METHOD IN CONCENTRIC STRATIFIED FIBER

In this section we will introduce a matrix method to compute the mode characteristics as well as the power flux of radially stratified fibers. The basic idea is to replace the boundary conditions by a matrix equation. Thus, each cladding interface is represented by a matrix. The introduction of this 4×4 matrix greatly simplifies the analysis.

We consider a fiber with the index profile given by

$$n(r) = \begin{cases} n_g, & 0 < r < r_1 \\ n_\nu, & r_\nu < r < r_{\nu+1} \\ \nu = 1,2,3,\ldots,\infty. \end{cases} \tag{1}$$

In particular, we will consider a fiber with a low-index core and alternating low- and high-index cladding. The geometry of this structure is sketched in Fig. 1. The index profile is then given by

$$n(r) = \begin{cases} n_g, & 0 \le r < r_1 \\ n_2, & r_1 \le r < r_2 \\ n_1, & r_2 \le r < r_3 \\ n_2, & r_3 \le r < r_4 \\ n_1, & r_4 \le r < r_5 \\ \vdots & \vdots \\ & \text{etc.} \end{cases} \tag{2}$$

We take the z axis as the direction of propagation, so that every field component has the form

$$\psi(r,\theta,z,t) = \psi(r,\theta)\, e^{i(\beta z - \omega t)}, \tag{3}$$

where ψ can be E_z, E_r, E_θ, H_z, H_r, H_θ. ω is the angular frequency and β is the propagation constant.

From waveguide theory we know that the transverse field components can be expressed in terms of E_z and H_z.[12]

$$E_r = \frac{i\beta}{\omega^2\mu\epsilon - \beta^2}\left(\frac{\partial}{\partial r}E_z + \frac{\omega\mu}{\beta}\frac{\partial}{r\partial\theta}H_z\right); \tag{4}$$

$$E_\theta = \frac{i\beta}{\omega^2\mu\epsilon - \beta^2}\left(\frac{\partial}{r\partial\theta}E_z - \frac{\omega\mu}{\beta}\frac{\partial}{\partial r}H_z\right); \tag{5}$$

$$H_r = \frac{i\beta}{\omega^2\mu\epsilon - \beta^2}\left(\frac{\partial}{\partial r}H_z - \frac{\omega\epsilon}{\beta}\frac{\partial}{r\partial\theta}E_z\right); \tag{6}$$

$$H_\theta = \frac{i\beta}{\omega^2\mu\epsilon - \beta^2}\left(\frac{\partial}{r\partial\theta}H_z + \frac{\omega\epsilon}{\beta}\frac{\partial}{\partial r}E_z\right). \tag{7}$$

$E_z(r,\theta)$ and $H_z(r,\theta)$ satisfy the wave equation

$$[\nabla_t^2 + (\omega^2\mu\epsilon - \beta^2)]\begin{Bmatrix} E_z \\ H_z \end{Bmatrix} = 0, \tag{8}$$

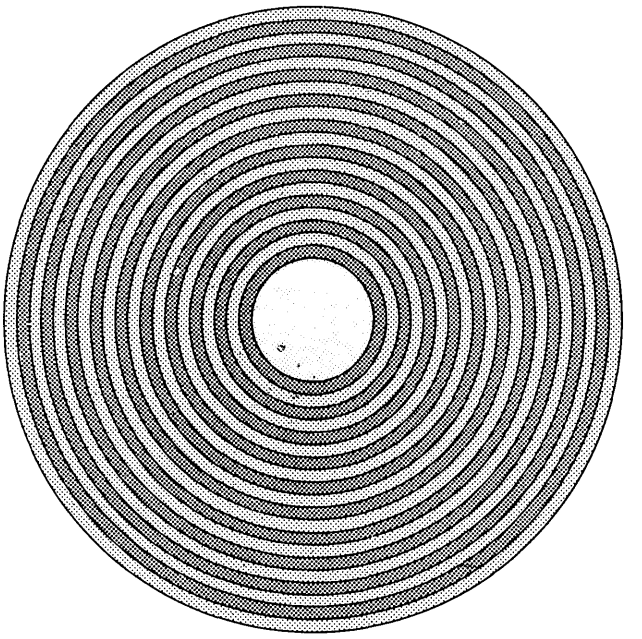

FIG. 1. Bragg fiber.

where $\nabla_t^2 = \nabla^2 - \partial^2/\partial z^2$ is the transverse Laplacian operator. The general solutions can be written

$$E_z = [AJ_l(kr) + BY_l(kr)]\cos(l\theta + \phi), \tag{9}$$

$$H_z = [CJ_l(kr) + DY_l(kr)]\cos(l\theta + \psi), \tag{10}$$

where A, B, C, C, ϕ, and ψ are constants, l is an integer, and

$$k = (\omega^2\mu\epsilon - \beta^2)^{1/2}. \tag{11}$$

We now consider the boundary conditions at a general cladding interface at $r = \rho$. The solution of the wave equation is taken as

$$E_z = [A_1J_l(k_1r) + B_1Y_l(k_1r)]\cos(l\theta + \phi_1), \quad r < \rho$$

$$E_z = [A_2J_l(k_2r) + B_2Y_l(k_2r)]\cos(l\theta + \phi_2), \quad r > \rho \tag{12}$$

and

$$H_z = [C_1J_l(k_1r) + D_1Y_l(k_1r)]\cos(l\theta + \psi_1), \quad r < \rho$$

$$H_z = [C_2J_l(k_2r) + D_2Y_l(k_2r)]\cos(l\theta + \psi_2), \quad r > \rho \tag{13}$$

where

$$k_i = [(\omega/c)^2\,\epsilon_i\mu_i - \beta^2]^{1/2}, \quad i = 1,2. \tag{14}$$

The boundary conditions at $r = \rho$ are that E_z, H_z, E_θ, and H_θ are continuous at the interface. Thus a 4×4 matrix can be found which relates A_1,B_1,C_1,D_1 to A_2,B_2,C_2,D_2, i.e.,

$$\begin{pmatrix} A_2 \\ B_2 \\ C_2 \\ D_2 \end{pmatrix} = M\begin{pmatrix} A_1 \\ B_1 \\ C_1 \\ D_1 \end{pmatrix}. \tag{15}$$

Derivation of M

In terms of fields (12) and (13) the continuity of E_z gives

$$[A_1J_l(k_1\rho) + B_1Y_l(k_1\rho)]\cos(l\theta + \phi_1) = [A_2J_l(k_2\rho) + B_2Y_l(k_2\rho)]\cos(l\theta + \phi_2). \tag{16}$$

This equation has to be satified for all θ which implies

$$\phi_1 = \phi_2 \tag{17}$$

and similarly from the continuity of H_z

$$\psi_1 = \psi_2. \tag{18}$$

Thus continuity of E_z and H_z gives

$$A_1 J_l(k_1\rho) + B_1 Y_l(k_1\rho) = A_2 J_l(k_2\rho) + B_2 Y_l(k_2\rho), \tag{19}$$

$$C_1 J_l(k_1\rho) + D_1 Y_l(k_1\rho) = C_2 J_l(k_2\rho) + D_2 Y_l(k_2\rho). \tag{20}$$

In terms of the fields (12), (13), and (5), the continuity of E_θ gives

$$\begin{aligned}\frac{1}{k_1^2}\Big(&\frac{-l}{\rho}\,[A_1 J_l(k_1\rho) + B_1 Y_l(k_1\rho)]\sin(l\theta+\phi) \\ &- \frac{\omega\mu_1}{\beta} k_1\,[C_1 J_l'(k_1\rho) + D_1 Y_l'(k_1\rho)]\cos(l\theta+\psi)\Big) \\ = \frac{1}{k_2^2}\Big(&\frac{-l}{\rho}\,[A_2 J_l(k_2\rho) + B_2 Y_l(k_2\rho)]\sin(l\theta+\phi) \\ &- \frac{\omega\mu_2}{\beta} k_2\,[C_2 J_l'(k_2\rho) + D_2 Y_l'(k_2\rho)]\cos(l\theta+\psi)\Big),\end{aligned} \tag{21}$$

where the primed quantities are the derivatives with respect to their own argument. Again, this equation has to be satisfied for all θ. From (19) and (20)

$$(1/k_1^2)\{A_1 J_l(k_1\rho) + B_1 Y_l(k_1\rho)\} \neq (1/k_2^2)[A_2 J_l(k_2\rho) + B_2 Y_l(k_2\rho)], \tag{22}$$

$$(\mu_1/k_1)[C_1 J_l'(k_1\rho) + D_1 Y_l'(k_1\rho)] \neq (\mu_2/k_2)[C_2 J_l'(k_2\rho) + D_2 Y_l'(k_2\rho)], \tag{23}$$

provided $k_1 \neq k_2$. Thus we conclude from (21)–(23) that

$$\sin(l\theta+\phi) = \pm\cos(l\theta+\psi) \tag{24}$$

or equivalently,

$$\phi = \psi \pm \pi/2. \tag{25}$$

Continuity of H_θ and Eq. (7) gives

$$\begin{aligned}\frac{1}{k_1^2}\Big(&\frac{-l}{\rho}\,[C_1 J_l(k_1\rho) + D_1 Y_l(k_1\rho)]\sin(l\theta+\psi) \\ &+ \frac{\omega\epsilon_1}{\beta} k_1\,[A_1 J_l'(k_1\rho) + B_1 Y_l'(k_1\rho)]\cos(l\theta+\phi)\Big) \\ = \frac{1}{k_2^2}\Big(&\frac{-l}{\rho}\,[C_2 J_l(k_2\rho) + D_2 Y_l(k_2\rho)]\sin(l\theta+\psi) \\ &+ \frac{\omega\epsilon_2}{\beta} k_2[A_2 J_l'(k_2\rho) + B_2 Y_l'(k_2\rho)]\cos(l\theta+\phi)\Big).\end{aligned} \tag{26}$$

From (24) or (25) we classify the waves into two categories:

$$\text{I}\qquad \begin{aligned}E_z &= [AJ_l(kr) + BY_l(kr)]\cos l\theta, \\ H_z &= [CJ_l(kr) + DY_l(kr)]\sin l\theta;\end{aligned} \tag{27}$$

$$\text{II}\qquad \begin{aligned}E_z &= [AJ_l(kr) + BY_l(kr)]\sin l\theta, \\ H_z &= [CJ_l(kr) + DY_l(kr)]\cos l\theta.\end{aligned} \tag{28}$$

The boundary conditions for these two categories are summarized below: For category I,

$$A_1 J_l(k_1\rho) + \quad B_1 Y_l(k_1\rho) + \quad 0 \quad + \quad 0 \quad = (1 \to 2), \tag{29}$$

$$\frac{\omega\epsilon_1}{k_1\beta} A_1 J_l'(k_1\rho) + \frac{\omega\epsilon_1}{k_1\beta} B_1 Y_l'(k_1\rho) + \frac{l}{k_1^2\rho} C_1 J_l(k_1\rho) + \frac{l}{k_1^2\rho} D_1 Y_l(k_1\rho) = (1 \to 2), \tag{30}$$

$$0 \quad + \quad 0 \quad + \quad C_1 J_l(k_1\rho) + \quad D_1 Y_l(k_1\rho) = (1 \to 2) \tag{31}$$

$$\frac{l}{k_1^2\rho} A_1 J_l(k_1\rho) + \frac{l}{k_1^2\rho} B_1 Y_l(k_1\rho) + \frac{\omega\mu_1}{k_1\beta} C_1 J_l'(k_1\rho) + \frac{\omega\mu_1}{k_1\beta} D_1 Y_l'(k_1\rho) = (1 \to 2), \tag{32}$$

where $(1 \to 2)$ means the same functional form with subscript 1 replaced by 2, and vice versa. For category II there are similar equations except that the coefficient $l/k_i^2\rho$ is replaced by $-l/k_i^2\rho$. Equations (29)–(32) can be written as a matrix equation

$$M(1,\rho)\begin{pmatrix}A_1\\B_1\\C_1\\D_1\end{pmatrix} = M(2,\rho)\begin{pmatrix}A_1\\B_2\\C_2\\D_2\end{pmatrix} \tag{33}$$

with

$$M(i,\rho) = \begin{bmatrix} J_l(k_i\rho) & Y_l(k_i\rho) & 0 & 0 \\ \frac{\omega\epsilon_i}{\beta k_i} J_l'(k_i\rho) & \frac{\omega\epsilon_i}{\beta k_i} Y_l'(k_i\rho) & \frac{l}{k_i^2\rho} J_l(k_i\rho) & \frac{l}{k_i^2\rho} Y_l(k_i\rho) \\ 0 & 0 & J_l(k_i\rho) & Y_l(k_i\rho) \\ \frac{l}{k_i^2\rho} J_l(k_i\rho) & \frac{l}{k_i^2\rho} Y_l(k_i\rho) & \frac{\omega\mu_i}{\beta k_i} J_l'(k_i\rho) & \frac{\omega\mu_i}{\beta k_i} Y_l'(k_i\rho) \end{bmatrix}, \tag{34}$$

where $i = 1,2$. We notice that when $l = 0$, the matrix is reducible. In other words, we can have pure TE or pure TM waves when $l = 0$.

The matrix in Eq. (15) can be written, using (33), as

$$M = M^{-1}(2,\rho)\, M(1,\rho). \tag{35}$$

If we define $x = k_1\rho$, $y = k_2\rho$, and write M as

$$M = \frac{\pi y}{2}\begin{pmatrix} m_{11} & m_{12} & m_{13} & m_{14} \\ m_{21} & m_{22} & m_{23} & m_{24} \\ m_{31} & m_{32} & m_{33} & m_{34} \\ m_{41} & m_{42} & m_{43} & m_{44} \end{pmatrix}. \tag{36}$$

Using (34) and after some matrix manipulation, the matrix elements m_{ij} in (36) are obtained as

$$
\begin{aligned}
m_{11} &= J_l(x)Y_l'(y) - (k_{2\epsilon_1}/k_{1\epsilon_2})J_l'(x)Y_l(y),\\
m_{12} &= Y_l(x)Y_l'(y) - (k_{2\epsilon_1}/k_{1\epsilon_2})Y_l'(x)Y_l(y),\\
m_{13} &= (\beta l/\omega\epsilon_2)(1/y - 1/x)J_l(x)Y_l(y),\\
m_{14} &= (\beta l/\omega\epsilon_2)(1/y - 1/x)Y_l(x)Y_l(y),\\
m_{21} &= (k_{2\epsilon_1}/k_{1\epsilon_2})J_l'(x)J_l(y) - J_l(x)J_l'(y),\\
m_{22} &= (k_{2\epsilon_1}/k_{1\epsilon_2})Y_l'(x)J_l(y) - Y_l(x)J_l'(y),\\
m_{23} &= (\beta l/\omega\epsilon_2)(1/x - 1/y)J_l(x)J_l(y),\\
m_{24} &= (\beta l/\omega\epsilon_2)(1/x - 1/y)Y_l(x)J_l(y),\\
m_{31} &= (\beta l/\omega\mu_2)(1/y - 1/x)J_l(x)Y_l(y),\\
m_{32} &= (\beta l/\omega\mu_2)(1/y - 1/x)Y_l(x)Y_l(y),\\
m_{33} &= J_l(x)Y_l'(y) - (k_{2\mu_1}/k_{1\mu_2})J_l'(x)Y_l(y),\\
m_{34} &= Y_l(x)Y_l'(y) - (k_{2\mu_1}/k_{1\mu_2})Y_l'(x)Y_l(y),\\
m_{41} &= (\beta l/\omega\mu_2)(1/x - 1/y)J_l(x)J_l(y),\\
m_{42} &= (\beta l/\omega\mu_2)(1/x - 1/y)Y_l(x)J_l(y),\\
m_{43} &= (k_{2\mu_1}/k_{1\mu_2})J_l'(x)J_l(y) - J_l(x)J_l'(y),\\
m_{44} &= (k_{2\mu_1}/k_{1\mu_2})Y_l'(x)J_l(y) - Y_l(x)J_l'(y).
\end{aligned}
\tag{37}
$$

Again we find that the transfer matrix M is block diagonalized when $l = 0$. In this case the matrix equation (15) can be written as two separate equations

$$\begin{pmatrix} A_2 \\ B_2 \end{pmatrix} = M_{\mathrm{TM}} \begin{pmatrix} A_1 \\ B_1 \end{pmatrix}, \tag{38}$$

$$\begin{pmatrix} C_2 \\ D_2 \end{pmatrix} = M_{\mathrm{TE}} \begin{pmatrix} C_1 \\ D_1 \end{pmatrix}. \tag{39}$$

The matrix method described above can be employed to obtain the mode dispersion relations for any conventional fibers. We will, however, use this technique to design a Bragg fiber in the next section.

III. BRAGG FIBERS

An optimization procedure similar to that of Ref. 5 will be introduced to design an optimum Bragg fiber. This procedure is to minimize the outflowing flux by properly choosing the thicknesses of the claddings. Without loss of generality we will consider TE modes ($l = 0$ and $E_z = 0$) only. The only nonvanishing components of the field for TE waves are

$$H_z = [CJ_0(kr) + DY_0(kr)]e^{i(\beta z - \omega t)}, \tag{40}$$

$$E_\theta = -\frac{i\omega\mu}{k^2}\frac{\partial}{\partial r}H_z, \tag{41}$$

$$H_r = \frac{i\beta}{k^2}\frac{\partial}{\partial r}H_z, \tag{42}$$

where C and D are constants. C and D are real in each layer because the field is normalized such that $H_z = e^{i(\beta_z - \beta t)}$ at $r = 0$. The radial component of the time averaged Poynting is given by

$$S_r = (1/2)\,\mathrm{Re}[E_\theta H_z^*] \tag{43}$$

$$= (1/2)\,\mathrm{Re}\,(-i\omega\mu/k)[CJ_0'(kr) + DY_0'(kr)] \times [C^*J_0(kr) + D^*Y_0(kr)]$$

$$= 0 \quad \text{for all } r. \tag{44}$$

This implies

$$\text{outflowing flux} = \text{inflowing flux}. \tag{45}$$

It can be shown that

$$\text{outflowing flux} = \text{inflowing flux} \propto (C^2 + D^2)\omega\mu/k^2. \tag{46}$$

Equation (44) is exactly true mathematically for the electromagnetic modes of our fiber structure either with a finite or infinite number of layers. This, however, does not mean that the propagation is lossless in a Bragg fiber of finite number of anular claddings. Mathematically, $S_r = 0$ means that these modes have standing-wave pattern in the radial direction. These standing-wave radiation modes can only be excited by an infinitely extended source.[13] It is thus obvious that in an actual experimental excitation of Bragg fiber modes of a finite Bragg fiber structure there is a net outward power flow because $(S_r)_{\mathrm{outward}}$ is not reflected and constitutes a loss. Therefore it is legitimate to calculate the loss based on the outflowing flux $(S_r)_{\mathrm{outward}}$.

Optimization of outflowing flux

Referring to Fig. 2, we consider the fields on both sides of a general cladding interface. The z component of magnetic field is taken as

$$H_z = \begin{cases} H_z(k_1 r), & r < \rho \\ CJ_0(k_2\rho) + DY_0(k_2\rho), & r > \rho \end{cases} \tag{47}$$

where $H_z(r)$ satisfies the wave equation

$$\left[\frac{1}{r}\frac{\partial}{\partial r}\left(r\frac{\partial}{\partial r}\right) - k_1^2\right]H_z(k_1 r) = 0 \tag{48}$$

and is determined by the boundary condition at $r = 0$. In terms of fields (40), (41), (42), and (47), the continuity of E and H_r gives

$$CJ_0(k_2\rho) + DY_0(k_2\rho) = H_z(k_1\rho) \equiv H(k_1\rho), \tag{49}$$

$$(\mu_2/k_2^2)[Ck_2J_0'(k_2\rho) + Dk_2Y_0'(k_2\rho)] = (\mu_1/k_1^2)k_1H_z'(k_1\rho) \equiv (\mu_1/k_1^2)k_1H'(k_1\rho), \tag{50}$$

where primed quantities are the derivatives with respect to their own argument. For the sake of simplicity in algebraic manipulation, we will drop the functional arguments and the z subscript. Thus we have

$$CJ_0 + DY_0 = H, \tag{51}$$

$$CJ_0' + DY_0' = (k_{2\mu_1}/\mu_2 k_1)H'. \tag{52}$$

Solving for C and D from (51) and (52) we obtain

$$C = (\pi k_2\rho/2)[HY_0' - (k_{2\mu_1}/k_{1\mu_2})Y_0H'], \tag{53}$$

$$D = (\pi k_2\rho/2)[(k_{2\mu_1}/k_{1\mu_2})J_0H' - J_0'H], \tag{54}$$

where we have used the Wronskian of Bessel functions

$$J_0(x)Y_0'(x) - J_0'(x)Y_0(x) = 2/\pi x. \tag{55}$$

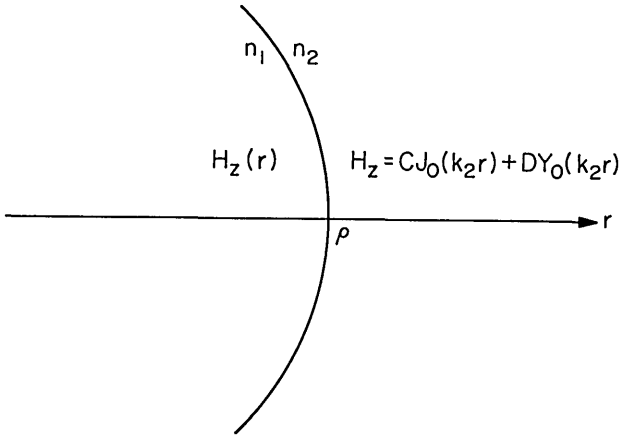

FIG. 2. General cladding interface at $r = \rho$.

The magnitude of C and D depends on the interface radius ρ. The purpose of optimization procedure is to find a ρ such that the outward flux (46) is a minimum.

$$\frac{\partial}{\partial \rho}(C^2 + D^2) = 0. \tag{56}$$

By carrying out the partial differentiation with respect to ρ, we obtain

$$\begin{aligned}\frac{\partial}{\partial \rho}(C^2 + D^2) = \frac{1}{2}\left(\frac{\pi k_2 \rho}{2}\right)^2 \Bigg\{\Bigg[k_2\left(\frac{\mu_1}{\mu_2} - 1\right) H^2 \\ - k_1 \frac{k_2\mu_1}{k_1\mu_2}\left(1 - \frac{k_2^2\mu_1}{k_1^2\mu_2}\right) H'^2\Bigg](J_0 J_0' + Y_0 Y_0') \\ + HH'\Bigg[k_1\left(1 - \frac{k_2^2\mu_1}{k_1^2\mu_2}\right)(J_0'^2 + Y_0'^2) \\ - k_2\left(\frac{\mu_1}{\mu_2} - 1\right)\frac{k_2\mu_1}{k_1\mu_2}(J_0^2 + Y_0^2)\Bigg]\Bigg\}. \end{aligned} \tag{57}$$

A similar expression can be obtained for TM waves by replacing H by E and μ_i by ϵ_i, $i = 1,2$.

Equation (57) is an exact general expression. If the fiber materials are pure dielectric, (57) can be simplified by using $\mu_2 = \mu_1$,

$$\begin{aligned}\frac{\partial}{\partial \rho}[C^2 + D^2] = \frac{1}{2}\left(\frac{\pi k_2 \rho}{2}\right)^2 \left(1 - \frac{k_2^2}{k_1^2}\right) \\ \times H'[k_1 H(J_0'^2 + Y_0'^2) - k_2 H'(J_0 J_0' + Y_0 Y_0')]. \end{aligned} \tag{58}$$

A further simplification can be made if we note that, for $x \gg 1$,

$$\frac{J_0(x)J_0'(x) + Y_0(x)Y_0'(x)}{J_0'^2(x) + Y_0'^2(x)} \sim O(1/x). \tag{59}$$

In practical application $x = k_2\rho$ is a large number (i.e., $k_2\rho \gg 1$) even in the first cladding interface. Therefore, the last term in (58) can be neglected. Thus we obtain

$$\begin{aligned}\frac{\partial}{\partial \rho}[C^2 + D^2] = \frac{1}{2}\left(\frac{\pi k_2 \rho}{2}\right)^2 \left(1 - \frac{k_2^2}{k_1^2}\right) \\ \times k_1[J_0'^2(k_2\rho) + Y_0'^2(k_2\rho)]\, H_z(k_1\rho) H_z'(k_1\rho). \end{aligned} \tag{60}$$

Equation (60) is similar to the corresponding equation for planar geometry.[5] The same conclusions are obtained that minimization occurs at $E_\theta = H_z' = 0$ if $k_2 > k_1$, and $E_\theta' = H_z = 0$ if $k_2 < k_1$. In a transition through the interface the field amplitude decreases by a factor of k_1/k_2 if $k_2 > k_1$ and $E_\theta = 0$. The field amplitude, however, does not increase for $k_2 < k_1$ provided the interface is located at the local maximum of E_θ, i.e., $E_\theta' = 0$. Thus by employing alternating claddings with different refractive indices, the field amplitude will decrease by a factor of k_1/k_2 per cladding pair, provided the interfaces are located according to the minimization procedure. As a result the field amplitude decreases exponentially as r increases. Theoretically, a confined mode is obtained if the alternating cladding is infinite. However, it is important to note that the field decay is nearly complete in several pairs of claddings so that practical structures with, say, ten pairs of claddings, are a good approximation to the infinite alternating claddings.

The calculated field distribution for a typical Bragg fiber-mode is shown in Fig. 3. We notice that each pair of claddings is exactly of "half-wave" thickness. The half-wave thickness of a given layer means that the transverse Bessel function field solution undergoes a full variation between two adjacent zeros in that thickness. Since the zeros of Bessel function are not equally spaced, the cladding thicknesses are not identical. However, they tend to become identical as r becomes large. This is due to the asymptotic form of the Bessel functions which approaches that of sine and cosine functions. The index profile shown in Fig. 3 looks almost periodic in the cladding region.

The leakage due to finite number of claddings will be discussed in Sec. IV.

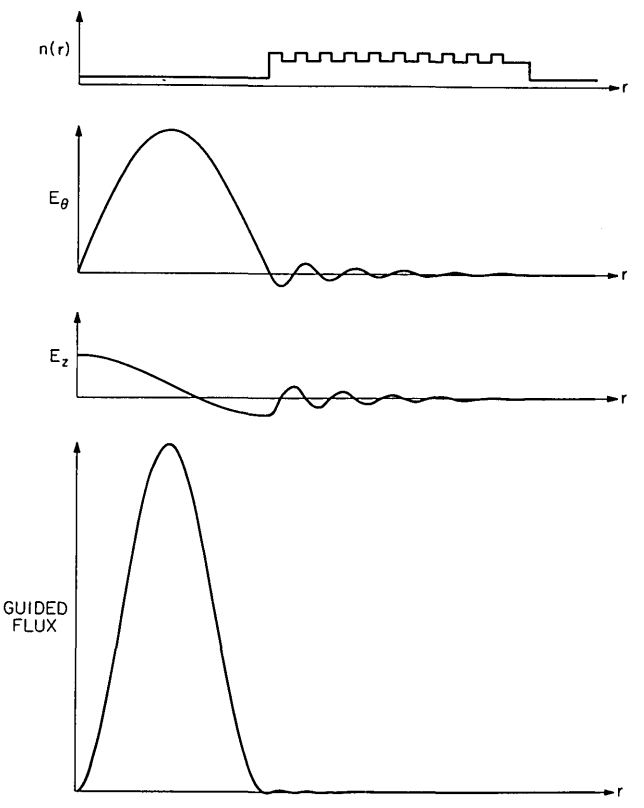

FIG. 3. Field distribution and guided flux of a typical Bragg fiber.

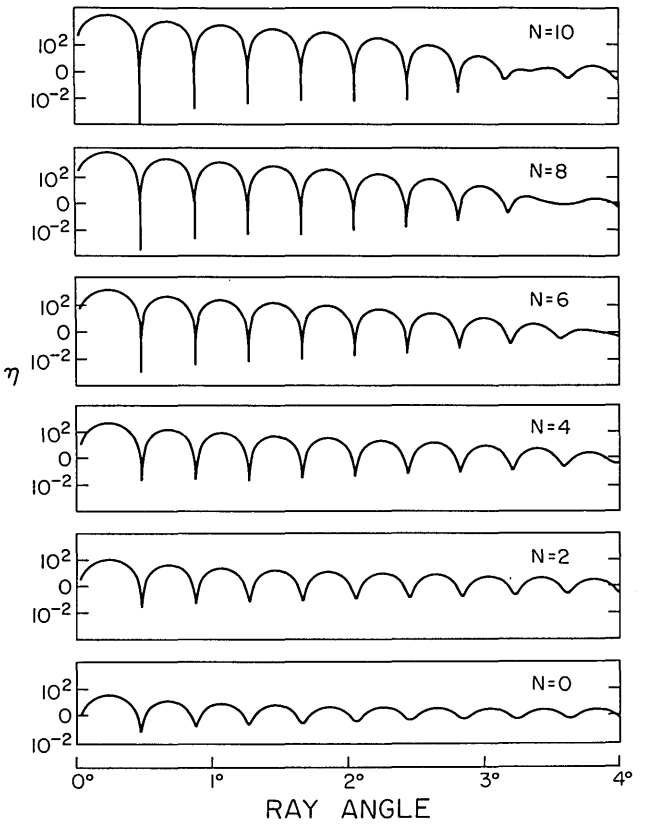

FIG. 4. Amplitude reduction factor η vs ray angle for $N = 0,2,4,6,8,10$.

IV. MODE CHARACTERISTICS AND LEAK CONSIDERATION

A Bragg fiber is usually designed to minimize the leakage for some particular mode. Again, we have the problem of leakage due to finite number of claddings. As a result, some higher-order undesired modes may be supported by the same Bragg fiber with larger attenuation coefficients. However, it can be shown numerically that these undesired modes are very lossy. Therefore, the Bragg fiber can be employed as a mode filter to select some particular mode from an ensemble of modes.

To study the mode characteristics and leakage problem, we start from a Bragg fiber structure optimized for some particular ray angle θ [or equivalently $\beta = (\omega/c)n\cos\theta$]. Then we study the amplitude reduction factor for any other ray angle θ. The amplitude reduction factor is defined as

$$\eta \equiv \frac{(C^2 + D^2)_{r=\infty}}{(C^2 + D^2)_{r=0}}. \tag{61}$$

This quantity is proportional to the ratio of the radial outward power flow in the last cladding region to the power flow in the core and is thus a direct measure of the attenuation coefficient α of the mode. (We can show that $\alpha \propto \eta$.) Given a Bragg fiber structure, η is a function of ray angle θ and number of pairs of claddings,

$$\eta = \eta(\theta,N). \tag{62}$$

Figure 4 shows the curves of η vs θ for various N's. The structure is optimized for the fundamental mode. The minima in the curves are virtual modes[14] of the structure. We see that the fundamental mode has the best degree of confinement. All the higher-order modes are less confined and hence more lossy. This is the basic property of a mode filter.

In conclusion, by extending the theory of Bragg reflection to cylindrical geometry we find that it is possible, in principle, to fabricate optical fibers with a multiannulus cladding whose indices may be higher than that of a core. Such fibers are strongly mode selective and can operate single mode even with large core diameter. A procedure for designing the optimum Bragg fibers is given and some of their properties discussed.

* Research supported by the NSF.

† Present address: Rockwell International Science Center, Thousand Oaks, CA 91360.

[1]P. Yeh and A. Yariv, Opt. Commun. **19,** 427 (1976).
[2]A. Y. Cho and J. R. Arthur, *Progress in Solid State Chemistry* (Pergamon, New York, 1975), Vol. 10, Part 3, pp. 157–191.
[3]A. Y. Cho, A. Yariv, and P. Yeh, Appl. Phys. Lett. **30,** 471 (1977).
[4]P. Yeh, A. Yariv, and C. S. Hong, J. Opt. Soc. Am. **67,** 423 (1977).
[5]P. Yeh, Ph.D. thesis (Caltech, 1977) (unpublished).
[6]D. Gloge, *Optical Fiber Technology* (IEEE, New York, 1975).
[7]E. Snitzer, J. Opt. Soc. Am. **51,** 491 (1961).
[8]E. Snitzer and H. Osterberg, J. Opt. Soc. Am. **51,** 499 (1961).
[9]A. Yariv, P. Yeh, and A. Y. Cho, "Guiding of Light in Bragg Configuration," presented at Device Research Conference, Ithaca, New York, June (1977).
[10]E. Garmire, T. McMahon, and M. Bass, Appl. Phys. Lett. **31,** 92 (1977).
[11]A. Yariv, Appl. Phys. Lett. **28,** 88 (1976).
[12]J. A. Stratton, *Electromagnetic Theory* (McGraw-Hill, New York, 1941).
[13]See, for example, D. Marcuse, *Theory of dielectric optical waveguides* (Academic, New York, 1974), p. 21.
[14]They are called virtual modes because their energy is more or less confined.